

# SERS of trititanate nanotubes: selective enhancement of catechol compounds

Ruochen Liu<sup>[a,b]</sup>, Edmund Morris<sup>[a,b]</sup>, Xiaorong Cheng<sup>[c]</sup>, Eric Amigues<sup>[a]</sup>, Kim Lau<sup>[a]</sup>, Baekman Kim<sup>[a]</sup>, Yuanhang Liu,<sup>[a]</sup> Zhipeng Ke,<sup>[d]</sup> Sharon E. Ashbrook,<sup>[d]</sup> Michael Bühl<sup>[d]</sup> and Graham Dawson<sup>\*[a]</sup>

**Abstract:** The surface enhanced Raman scattering of trititanate nanotubes (TiNT) modified with enediol ligands was investigated and it was found that the functional group dramatically affects the enhancement observed. For TiNT-4-nitrocatechol, a SERS enhancement is seen; however, when dopamine is attached, no signal is seen. The relative band gap positions upon 785 nm laser excitation are proposed to explain the observed phenomenon. This attachment is investigated by solid state NMR and UV/Vis spectroscopy and supported by DFT calculations to offers further insights into catechol coatings of nanomaterials and SERS by the chemical method. We expect this non noble metal containing composite material to have applications in bioimaging and bio and chemical detection.

## Introduction

Semiconducting inorganic nanostructures<sup>[1, 2]</sup> have been extensively investigated for applications in photocatalysis, energy storage and biomedical probes. Within this field, TiO<sub>2</sub> has received considerable of interest due to its photocatalytic properties<sup>[3, 4]</sup>, which include high oxidative power and long term stability. In 1998, Kasuga *et al.* reported the preparation of titania nanotubes<sup>[5]</sup> through the hydrothermal treatment of TiO<sub>2</sub> with 10 M NaOH. These nanotubes had a porous structure and high surface area. The composition of the nanotubes was subsequently identified as trititanate<sup>[6-9]</sup>, H<sub>2</sub>Ti<sub>3</sub>O<sub>7</sub>. We have modified these nanotubes with dopamine, which imbued the nanotubes with photocatalytic properties. This caused the promotion of electron injection and charge separation and added activity to the unmodified system<sup>[10]</sup>. The modification resulted in a colour change and a shoulder in the UV-vis spectrum, stemming from the created charge transfer complex. With a view to biomedical applications, this was further investigated using

ssNMR and XRD to discern if any degree of polymerisation had occurred. Our study found that the dopamine molecules attached as monomer units through either a monodentate or bidentate mode of binding<sup>[11]</sup>.

Surface enhanced Raman scattering (SERS) is a powerful analytical technique for chemical sensing of trace amounts of analyte, providing in-depth structural information. Most SERS results published to this date have used metallic, particularly silver and gold, nanoparticles and the enhancement has come from a mixture of the surface plasmon resonance of the metal nanoparticles and a charge transfer resonance involving the transfer of electrons between the molecule and the conduction band of the metal. A third contribution comes from the resonances within the molecule itself- the chemical method,<sup>[12]</sup> however the exact mechanism is still a source of debate. Semiconductor SERS has been reported<sup>[13, 14]</sup> for TiO<sub>2</sub> as well as other semiconductors<sup>[15, 16]</sup>. The chemical method requires a specific interaction between the adsorbed molecules and the surface, and forms a charge transfer complex which absorbs light at the excitation wavelength, producing resonance Raman scattering<sup>[13]</sup>. The plasmon resonance frequency of most semiconductors is either in the infrared region or of poor quality due to coupling between the conduction electrons and the interband electronic transitions<sup>[17]</sup>, however this type of SERS has been shown for TiO<sub>2</sub> nanoparticles modified with enediol catechol ligands<sup>[13, 14]</sup>. In this system nontotally symmetric vibrations lead to deviations in the symmetry of the modifier and are necessary for the charge transfer transitions and, therefore, the surface enhancement.

The chemical method of SERS is often described by the photo-induced charge transfer (PICT) process, however when a surface complex is involved the Surface Complexes Resonance Enhancement mechanism is the most appropriate explanation. Complexes formed by the chemisorption of molecules on the substrate surface form new highest occupied molecular orbital (HOMO) and lowest unoccupied molecular orbitals (LUMO), which under suitable excitation show resonance Raman scattering enhancement<sup>[18, 19]</sup>.

The investigation into the SERS properties of various enediol ligands attached to trititanate nanotubes has shown interesting results. These nanotubes have a scroll structure with a diameter of 8 nm and lengths of in excess of 100 nm. We see a dependence on the SERS effect related to the proximity of the functional group to the benzene ring for this system. This study offers further insights into catechol coatings of nanomaterials and SERS by the chemical method. We expect this composite material to have applications in bioimaging<sup>[20, 21]</sup> and in bio and chemical<sup>[22, 23]</sup> detection where the biocompatible nature of the system will be an advantage.<sup>[24, 25]</sup>

[a] Mr. R. Liu, Mr. E. Morris, Dr. E. Amigues, Prof. K. Lau, Mr. B. Kim, Mr. Y. Liu and Dr. G. Dawson  
Department of Chemistry  
Xian Jiaotong Liverpool University, Suzhou, PR China  
E-mail: [graham.dawson@xjtu.edu.cn](mailto:graham.dawson@xjtu.edu.cn)

[b] Mr. R. Liu, Mr. E. Morris  
Department of Chemistry  
University of Liverpool, Crown Street Liverpool

[c] Dr. X. Cheng  
Suzhou Institute of Industrial Technology  
Suzhou, PR China

[d] Mr. Z., Ke, Prof. S. E. Ashbrook, Prof. M. Bühl  
School of Chemistry, University of St Andrews  
Supporting information for this article is given via a link at the end of the document.

## Results and Discussion

In our previous work we have proposed mixed bidentate and monodentate *in-situ* structural models for dopamine on trititanate nanotubes using solid state NMR and powder XRD. The dopamine monomer units exist in a close packed arrangement on the nanotube surface<sup>[11]</sup>. We have previously shown this system to be photocatalytically active<sup>[10]</sup>. In this current work we have examined the surface enhanced Raman activity of a series of enediol functionalized TiNT systems. The position of the sidechain/functional group is of paramount importance to the SERS effect. Figure 1 shows the solid drs UV/vis of TiNT

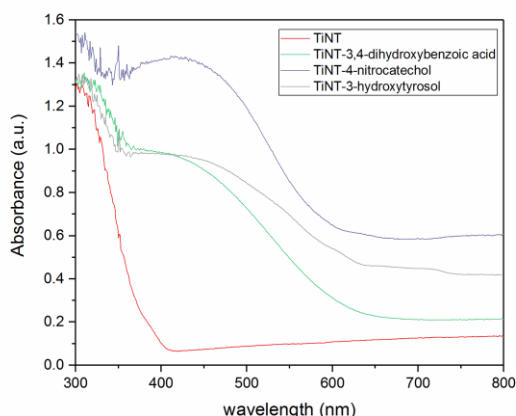


Figure 1. UV/vis spectra for TiNT and TiNT-modified samples

functionalized by various enediol ligands. As can be observed, all samples show a similar profile: a charge transfer<sup>[13]</sup> band dominating the visible range of the spectrum with an onset from 600 nm and showing a shoulder leading into the band edge at around 380 nm. The intensity of the shoulder is greatest for the 4-nitrocatechol modified sample, however all samples show a similar profile indicating a similar attachment mode for all compounds, which is expected from this selection of organic modifiers. The colour of the samples can be seen in SF1. Our calculations have confirmed the existence of charge transfer complexes and will be discussed later.

**Solid state NMR:** <sup>13</sup>C NMR spectra of the modified samples showed attachment through a bidentate or monodentate Ti-O-aromatic C, as previously observed for TiNT-dopamine<sup>[11]</sup>. This is shown in Figure 2 for TiNT- 4-nitrocatechol (a), TiNT-3-hydroxytyrosol (b) and TiNT-3,4-dihydroxybenzoic acid (c). In all cases a peak shift to higher ppm values was observed upon functionalization caused by the replacement of C-OH bonds by C-OH-Ti bonds. These findings are corroborated by computation of the <sup>13</sup>C NMR chemical shifts of the parent catechol (free and attached to a Ti<sub>10</sub>O<sub>20</sub> model cluster, see ESI). These results show that the best fit with the experimental data comes for the configuration that retains one OH group upon binding to the nanotube surface, and is not fully deprotonated. Furthermore, we observed downshifting of an aromatic C signal, ascribed to  $\pi$ - $\pi$  stacking of the dopamine monomers on the nanotube surface. This is also seen for 3,4-dihydroxybenzoic acid, 3-hydroxytyrosol and 4-nitrocatechol.  $\pi$ - $\pi$  stacking is supported by the XRD patterns shown in figure SF2.

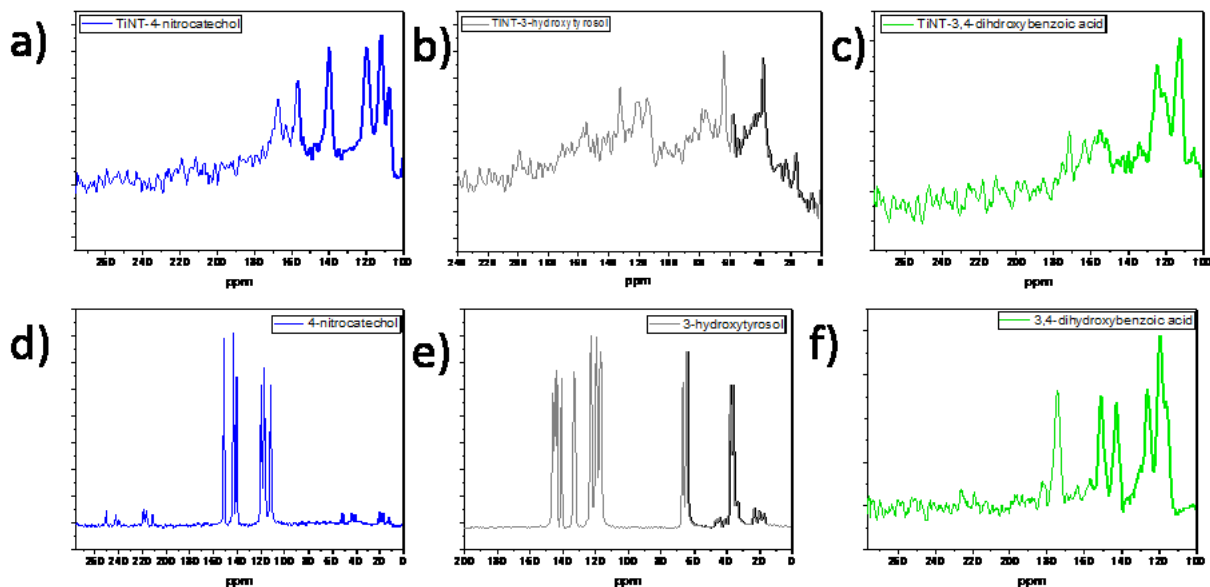
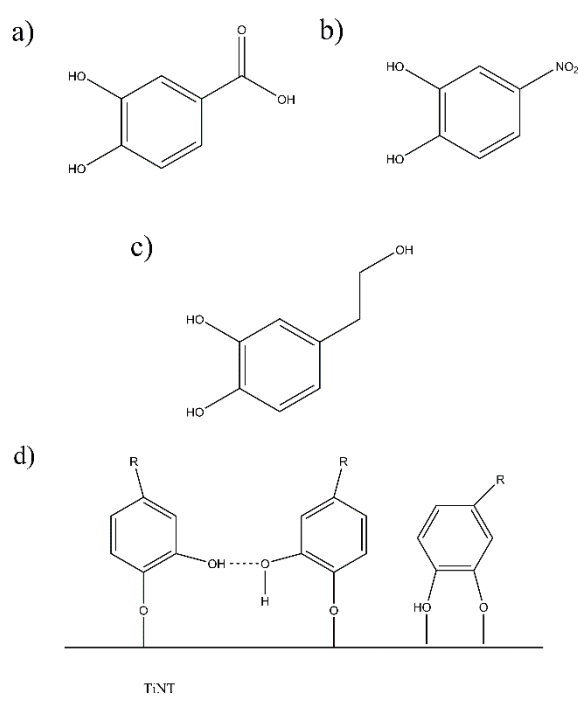


Figure 2 ssNMR spectra of the TiNT-modified samples (a-c) and the starting materials (d-f).

For the starting material 4-nitrocatechol, shown in Figure 2 (d), the  $^{13}\text{C}$  NMR signals are assigned as follows: the two carbon atoms attached to the hydroxyl groups at  $\delta = 143.2$  and  $151.1$  ppm, the nitro functionalized carbon at  $\delta = 140.4$  ppm and the other three aromatic carbon atoms at  $\delta = 111.6$ ,  $117.2$  and  $119.6$  ppm. Upon functionalization the two hydroxyl carbon signals show a shift to larger ppm values, indicating conversion of the C-OH to C-O-Ti bonds,  $156.8$  and  $167.2$  ppm. From our computation of the  $^{13}\text{C}$  NMR chemical shifts we can conclude that the 4-nitrocatechol is not fully deprotonated upon binding to titanate surfaces, but most likely retains one of the OH groups (see Figure S12 and S13). The aromatic carbon signals appear at  $\delta = 107.6$ ,  $111.8$  and  $120.1$  ppm in the product, all downshifted compared to the starting material. The peak at  $\delta = 140.2$  ppm is assigned as the C attached to the nitro group on the aromatic ring.



**Figure 3.** (a-c) structures of organic modifiers and (d) proposed general modes of attachment

For the starting material 3-hydroxytyrosol, shown in Figure 2 (e), the  $^{13}\text{C}$  NMR are assigned as follows: the carbon atoms in the chain  $\delta = 37.8$  and  $64.2$  ppm, the two carbon atoms attached to the hydroxyl groups at  $\delta = 143.5$  and  $144.9$  ppm, the chain functionalized carbon at  $\delta = 133$  ppm and the other three aromatic carbon atoms at  $\delta = 116.8$ ,  $119.2$  and  $122.7$  ppm. Upon functionalization the two hydroxyl carbon signals show a shift to larger ppm values, indicating conversion of the C-OH to C-O-Ti bonds,  $154.8$  and  $156.8$  ppm. The aromatic carbon signals appear at  $\delta = 114.8$ ,  $120.8$  and  $132.6$  ppm in the product. The carbon with the lowest ppm signal downshifted from  $\delta = 116.8$  to  $114.8$  ppm.

The carbons on the chain are still present, as is also true for dopamine modification, showing that no cyclisation has occurred. For the starting material 3,4-dihydroxybenzoic acid, shown in Figure 2 (f), the  $^{13}\text{C}$  NMR signals are assigned as follows: the carbon atom in the carboxylic acid group  $\delta = 174.7$  ppm, the two carbon atoms attached to the hydroxyl groups at  $\delta = 151.5$  and  $143.1$  ppm, and the four other aromatic carbon atoms at  $\delta = 126$  (overlapping 2 peaks),  $119.6$  and  $116.5$  ppm. Upon functionalization the carboxylic acid group signal is downshifted to  $171.6$  ppm. The two hydroxyl carbon signals show a shift to larger ppm values, indicating conversion of the C-OH to C-O-Ti bonds,  $156$  and  $163.6$  ppm. The aromatic carbon signals are all downshifted to  $\delta = 124.8$ ,  $121$ ,  $112$  and  $105$  ppm.

For the three structures shown in Figure 3, structures a-c, ssNMR and XRD show attachment through the proposed mechanism depicted generally in Figure 3 d.

**Surface Enhanced Raman Scattering:** SERS is mainly observed with metallic nanoparticles, however it has been shown to occur on semiconductors.<sup>[15,16]</sup> Furthermore, Rajh and coworkers have shown SERS on  $\text{TiO}_2$  nanoparticles attached to enediol ligands<sup>[13,14]</sup>, which occurs through the formation of a charge transfer complex. We have observed a similar enhancement on TiNT, although the enhancement is dependent on the structure of the enediol organic ligand. The formation of charge transfer complexes for all modifiers is indicated by the UV/vis spectra; the computed HOMO and LUMO positions of TiNT modified with catechol, 4-nitrocatechol and protonated dopamine are shown in Figure 4. The values of band gaps are  $1.35$  eV,  $1.62$  eV and  $1.88$  eV respectively. The Raman laser used in the experiments had a wavelength of  $785$  nm, which corresponds to  $1.58$  eV. Our experiments show that the TiNT-4-nitrocatechol system displays a SERS enhancement, but that the TiNT-dopamine system does not. It is reasonable the excitation wavelength of the laser does not have enough energy to promote electrons across the band gap for the TiNT-dopamine system, (Note, however, that the computed band gap depends on the protonation state and presence of counterions, see Figure S9) resulting in no SERS effect for this system, but showing a SERS enhancement for the TiNT-4-nitrocatechol system. Without the organic modification the band gap of the TiNT system is  $3.4$  eV, much too large to be excited by the  $785$  nm laser directly<sup>[18,26]</sup>.

As can be seen in Figure 5 a and b, an enhanced Raman signal is observed for TiNT-4-nitrocatechol and TiNT-3,4-dihydroxybenzoic acid. We also expected to see an enhancement for the TiNT-dopamine and TiNT-3-hydroxytyrosol systems as they had shown similar optical profiles in the UV-vis spectra; in fact, no distinguishable peaks were observed and this is explained by the calculated band gaps.

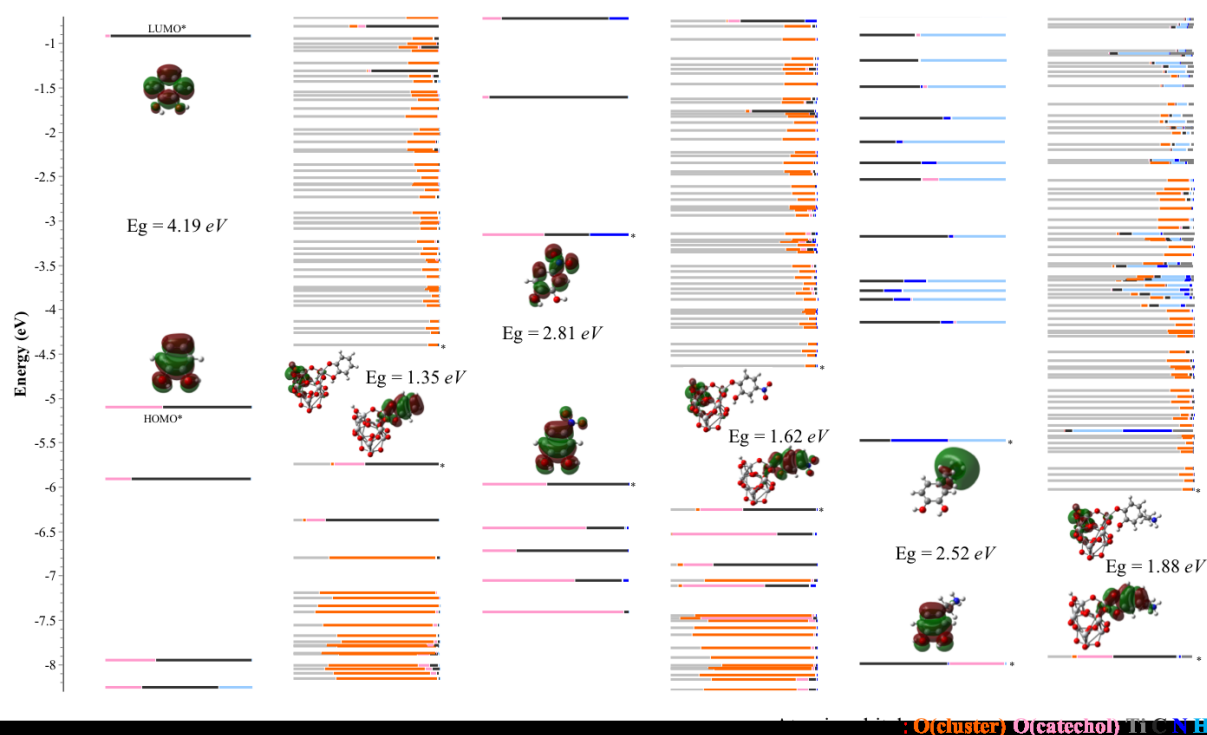


**Figure 4.** Molecular orbital scheme for dopants and the molecular models of dopants on TiNT (PBE level).

Both the nitro and carboxylic acid substituents are electron withdrawing groups. The nitro group is a strong electron withdrawing group, whilst the carboxylic acid group is a moderate electron withdrawing group. The alkyl side chains are weak electron donating groups. This trend matches our computation results of calculated band gaps shown in Figure 4. The UV/Vis spectra does not change significantly between samples.

As a result of different substituent groups on the catechol ring, different electron densities, dipole moments and polarizability will be observed in the charge transfer complex. A greater electron withdrawing effect has shown a larger SERS enhancement in the para position in mercapto benzene derivatives<sup>[19]</sup>.

For TiNT-3,4-dihydroxybenzoic acid, five high intensity, sharp peaks are observed. Similar peaks are observed for TiNT-4-nitrocatechol, shown in Table 1. In both Raman spectra that show an enhancement, the bands can be assigned<sup>[27-29]</sup> as the phenolate C-O stretch ( $\sim 1279\text{ cm}^{-1}$ ,  $\nu_{CO}$ ), stretching between the two hydroxyl carbons ( $\sim 1482\text{ cm}^{-1}$ ,  $\nu_{19b}$ ) and skeletal modes of the benzene ring ( $\sim 1330\text{ cm}^{-1}$ ,  $\nu_3$ ,  $1430\text{ cm}^{-1}$   $\nu_{19a}$  and  $1584\text{ cm}^{-1}$ ,  $\nu_{8a}$  combined  $\nu_{8b}$ ).

Bands that show enhancement for TiNT-3,4-dihydroxybenzoic acid are in the range of  $1100$  to  $1600\text{ cm}^{-1}$ , which are the modes associated with ligand to metal charge transfer<sup>[13,27,28]</sup>. The peak observed in both functionalized nanotube samples at around  $820\text{ cm}^{-1}$  is interesting. A peak is observed in 4-nitrocatechol around this wavenumber, and is assigned as a  $\text{NO}_2$  bend. There is no peak observed in 3,4-dihydroxybenzoic acid or the unmodified nanotubes around this

wavenumber, although the same peak is observed in both modified samples. The appearance of this band suggests that upon attachment of the modifier to the nanotube surface the symmetry of the surface is altered, allowing this band to be observed, and is therefore proposed to be Ti-O-Ti framework stretching.

**Table 1.** Raman peaks and assignments

TiNT- +		$\nu_{CO}$	$\nu_3$	$\nu_{19a}$	$\nu_{19b}$
3,4-dihydroxybenzoic acid	825	1279	1334	1431	1487
4-nitrocatechol	818	1278	1322	1419	1474

Transmission electron microscope (TEM) images shown in Figure SF4 are representative of the modified nanotubes, and show a thin amorphous coating of 1-2 nm. The thermogravimetric analysis (TGA) and CHN analysis for the three modified materials is shown in table ST1. The surface coverages are calculated assuming a coverage of  $19.6\text{ \AA}^2$  for the enediol ligands, with a BET surface area of  $249.4\text{ m}^2/\text{g}$ . The internal surface area of the nanotube will not be available for functionalization, resulting in the observed external surface coating. All samples have a surface coverage on the same order of magnitude, ranging from 12 to 6%. Also shown in Figure 5 a and b are the Raman signals observed for 3,4-dihydroxybenzoic acid and 4-nitrocatechol at concentrations of 0.1 M. This concentration equates to a wt% of 1.5% for the two

modifiers, which is of a similar magnitude to the modified TiNT samples. Compared to this concentration, the enhancement of signal is  $\sim 10$  fold for TiNT-3,4-dihydroxybenzoic acid and  $\sim 75$  fold for TiNT-4-nitrocatechol. In Figure 5 c we can observe the Raman spectra for the unmodified TiNT along with the spectra for

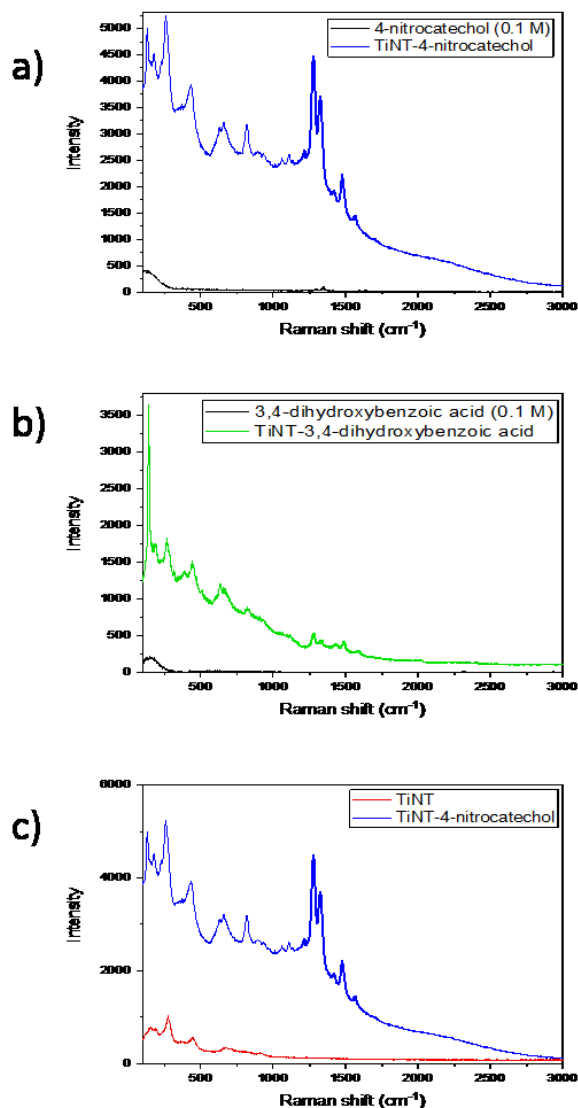


**Figure 5.** (a) and (b) Raman spectra for modified TiNT, modifier spectra without TiNT also shown for comparison. (c) Raman spectra of TiNT and TiNT-4-nitrocatechol.

TiNT-4-nitrocatechol, which also confirms that the enhancement in signal is due to the attached organic modifier.

The enlarged Raman spectra for 0.1 M 3,4-dihydroxybenzoic acid is shown in Figure SF3 for reference.

## Conclusions

In this study the structure and SERS enhancement of trititanate nanotubes modified with enediol ligands was investigated, and it was found that the functional group dramatically affects the enhancement observed. When 4-nitrocatechol and 3,4-dihydroxybenzoic acid were attached to the nanotubes, a functional group attached directly to the benzene ring, a SERS enhancement is seen. In contrast, when the functional group is attached via a carbon chain, in the case of 3-hydroxytyrosol and dopamine, no signal is seen. Calculated band gaps for the TiNT-4-nitrocatechol and TiNT-dopamine systems suggest that the laser energy is the limiting factor in whether a SERS enhancement is seen. The attachment was investigated by solid state NMR and UV/Vis spectroscopy and offers further insights into catechol coatings of nanomaterials and SERS by the chemical method.

## Experimental Section

**Materials:** Titanium dioxide (anatase) and dopamine hydrochloride were purchased from Sigma-Aldrich. 4-Nitrocatechol, 3,4-Dihydroxybenzoic acid and 3-Hydroxytyrosol were purchased from Aladdin. Structures are shown in Figure 3 a-c. Clear glass microscope slides were purchased from Fisher Scientific.

**Instrumentation:** UV-Vis absorbance spectrum were recorded using Cary 300 UV-Vis for solid samples, and Cary 60 Uv-Vis for liquid samples.  $^{13}\text{C}$  solid state NMR spectra were measured on a Bruker Advance III 400 spectrometer equipped with a 4 mm H/X DVT probe. CHN Element Analysis were measured on an Elementar vario MACRO CHNS. Powder X-ray diffraction was recorded on a Bruker D8 advance diffractometer with  $\text{Cu K}\alpha$  at 40 kV and 40 mA. Transmission electron microscope (TEM) images were carried out on a FEI Tecnai F20 operating at 200 kV.

**Synthesis:** Synthesis of TiNT was carried out based on the literature procedure<sup>[30]</sup>: anatase  $\text{TiO}_2$  (1 g) was added into a 10 M NaOH solution (20 mL). The resulting slurry was transferred to a TEFLON vessel, and put into a hydrothermal autoclave maintained at 140 °C for 72 hours. The autoclave was then cooled under running water. The white solid was removed and washed with water, 1 M HCl solution and finally with large amount of water until the pH value of the effluent was neutral. Surface modification of TiNT. Typically, TiNT was suspended in MilliQ water, then 10 wt% of organic compound was added. For TiNT-3,4-dihydroxybenzoic acid, TiNT-4-Nitrocatechol and TiNT-3-hydroxytyrosol, the mixture was stirred at room temperature overnight. The resulting solid was removed, washed with water and ethanol in order to remove any excess ligand.

**Raman Experiments:** Raman measurements were made using HORIBA Scientific XploRA. For solid samples, the powder was put on the centre of glass slide, focused by microscope. For liquid samples, a flat metal plate was firstly measured as background. Several drops of liquid samples were dropped on the centre of metal plate, focused by laser, and were measured immediately to minimize the effects of evaporating. A 785 nm laser was

used for excitation. Typical spectra acquisition parameters were: laser: 785nm; Filter: 100%; Hole: 300; Slit: 100; Grating: 1200T; RTD exposure time: 1s; Exposure time: 5s; Accumulation number: 3. Experiments were repeated several times on the same sample, and spectra shown are representative and reproducible.

## Computational details

Non-periodic calculations were carried out using Gaussian 09 (Gaussian 09, Revision B.01)<sup>[31]</sup>. Structures were fully optimized at the B3LYP level<sup>[32]</sup>, employing 6-31G\*<sup>[33]</sup> basis on the dopants (catechol, dopamine and 4-nitrocatechol), the LanL2DZ pseudopotential<sup>[34]</sup> and associated valence basis on Ti, and 6-31G<sup>[35]</sup> on the remaining O atoms of the cluster. Computed harmonic vibrational frequencies were all real indicating the optimized structures are true minima. The structures were then re-optimized at the dispersion-corrected B3LYP-D3 level<sup>[36]</sup>. A small Ti<sub>10</sub>O<sub>20</sub> cluster from the literature<sup>[37]</sup> was used as a model for TiNT surfaces. The catechol derivatives were added to one Ti site and a few selected tautomeric forms with H atoms placed on different positions of the cluster were explored. Invariably, a singly deprotonated catechol moiety with that proton attached to an O atom of the cluster was most stable (see Figures S5-S8 in the ESI). Because dopamine is used in form of its hydrochloride, the N atom was protonated in the calculations (see ESI for non-protonated and zwitterionic models with counterion). Single point calculations were performed using the B3LYP-D3 structures, PBE functional<sup>[38]</sup>, the same LANL2DZ/6-31G basis set/pseudopotential on TiO<sub>2</sub>, and a larger basis set (IGLO-II, designed originally for NMR parameters<sup>[39]</sup>) on dopants.

## Acknowledgements

This work is supported by Xi'an Jiaotong Liverpool University research development fund (RDF- RDF-16-01-06), SURF projects and National Natural Science Foundation of China (Grant No. 21650110446). MB thanks EaStCHEM for support and access to a computing facility maintained by H. Früchtl. ZK gratefully acknowledges a scholarship from the Chinese Scholarship Council. SEA thanks the EPSRC for support (EP/M022501/1).

**Keywords:** SERS • nanotubes • surface modification

- [1] R. Tenne, L. Margulis, M. Genut, G. Hodes, *Nature*, **1992**, *360*, 444-446.
- [2] Y. Feldman, E. Wasserman, D. J. Srolovitz, R. Tenne, *Science*, **1995**, *267*, 222-225.
- [3] P. Hoyer, *Langmuir*, **1996**, *12*, 1411-1413.
- [4] A. Fujishima, K. Hashimoto, T. Watanabe, *TiO<sub>2</sub> Photocatalysis: Fundamentals and applications*, BKC, Tokyo, **1999**.
- [5] T. Kasuga, M. Hiramatsu, A. Hoson, T. Sekino, K. Niihara, *Langmuir*, **1998**, *14*, 3160-3163.
- [6] A. Thorne, A. Kruth, D. Tunstall, J.T.S. Irvine, W. Zhou, *J. Phys. Chem. B.*, **2005**, *109*, 5439-5444.
- [7] Q. Chen, W. Zhou, G. Du, L.-M. Peng, *Adv. Mater.*, **2002**, *14*, 1208-1211.
- [8] S. Zhang, L.-M. Peng, Q. Chen, G.H. Du, G. Dawson, W. Zhou, *Phys. Rev. Lett.*, **2003**, *91*, 256103.
- [9] D. V. Bavykin, J. M. Friedrich, F. C. Walsh, *Adv. Mater.*, **2006**, *18*, 2807-2824.
- [10] G. Dawson, J. Liu, L. Lu, W. Chen, *ChemChatChem*, **2012**, *4*, 1133-1138.
- [11] R. Liu, X. Fu, C. Wang, G. Dawson, *Chem. Eur. J.*, **2016**, *22*, 6071-6074.
- [12] J. R. Lombardi, R. L. Birke, *Acc. Chem. Res.*, **2009**, *42*, 734-742.
- [13] S. J. Hurst, H. C. Fry, D. J. Gosztola, T. Rajh, *J. Phys. Chem. C*, **2011**, *115*, 620-630.
- [14] A. Musumeci, D. Gosztola, T. Schiller, N. M. Dimitrijevic, V. Mujica, D. Martin, T. Rajh, *J. Am. Chem. Soc.*, **2009**, *131*, 6040-6041.
- [15] Hayashi, R. Koh, Y. Ichiyama, K. Yamamoto, *Phys. Rev. Lett.*, **1988**, *60*, 1085-1088.
- [16] Y. Wang, Z. Sun, H. Hu, S. Jing, B. Zhao, W. Xu, C. Zhao, J. R. Lombardi, *J. Raman Spectrosc.*, **2007**, *38*, 34-38.
- [17] Z. Q. Tian, B. Ren, D. Y. Wu, *J. Phys. Chem. B*, **2002**, *106*, 9463-9483.
- [18] X. Wang, W. Shi, G. She, L. Mu, *Phys. Chem. Chem. Phys.*, **2012**, *14*, 5891-5901.
- [19] L. Yang, X. Jiang, W. Ruan, B. Zhao, W. Xu, J. R. Lombardi, *J. Phys. Chem. C*, **2008**, *112*, 20095-20098.
- [20] V. Biju, *Chem. Soc. Rev.*, **2014**, *43*, 744-764.
- [21] J. Cai, V. Raghavan, Y. J. Bai, M. H. Zhou, L. Liu, C. Y. Liao, P. Ma, L. Shi, P. Dockery, I. Keogh, H. M. Fan, M. Olivo, *J. Mater. Chem. B*, **2015**, *3*, 7377-7385.
- [22] J. Chao, W. Cao, S. Su, L. Weng, S. Song, C. Fan, L. Wang, *J. Mater. Chem. B*, **2016**, *4*, 1757-1769.
- [23] X. Zhu, Y. Liu, P. Li, Z. Nie, J. Li, *Analyst*, **2016**, *141*, 4541-4553.
- [24] K. Huo, B. Gao, J. Fu, L. Zhao, P. K. Chu, *RSC Adv.*, **2014**, *4*, 17300-17324.
- [25] J. Y. Huang, Y. K. Lai, F. Pan, L. Yang, H. Wang, K. Q. Zhang, H. Fuchs, L. F. Chi, *Small*, **2014**, *10*, 4865-4873.
- [26] P. Tarakeshwar, D. Finkelstein-Shapiro, T. Rajh, V. Mujica, *Int. J. Quant. Chem.*, **2011**, *111*, 1659-1670.
- [27] N. S. Lee, Y. Z. Hsieh, R. F. Paisley, M. D. Morris, *Anal. Chem.*, **1988**, *60*, 442-446.
- [28] S. Salama, J. D. Stong, J. B. Niellands, T. G. Spiro, *Biochemistry*, **1978**, *17*, 3781-3785.
- [29] J. P. Cornard, Rasmiwetti, J. C. Merlin, *Chem. Phys*, **2005**, *309*, 239-249.
- [30] G. Dawson, W. Chen, Z. Zhang, Z. Chen and X. Cheng, *Solid State Sciences*, **2010**, *12*, 2170-2176.
- [31] M. J. Frisch, G.W. Trucks, H. B. Schlegel, G. E. Scuseria, M.A. Robb, J. R. Cheeseman, G. Scalmani, V. Barone, B. Men- nucci, G. A. Petersson, H. Nakatsuji, M. Caricato, X. Li, H. P. Hratchian, A. F. Izmaylov, J. Bloino, G. Zheng, J.L. Sonnenberg, M. Hada, M. Ehara, K. Toyota, R. Fukuda, J. Hasegawa, M. Ishida, T. Nakajima, Y. Honda, O. Kitao, H. Nakai, T. Vreven, J. A. Montgomery, J.E. Peralta, F. Ogliaro, M. Bearpark, J. J. Heyd, E. Brothers, K. N. Kudin, V. N. Staroverov, T. Keith, R. Kobayashi, J. Normand, K. Raghavachari, A. Rendell, J. C. Burant, S.S. Iyengar, J. Tomasi, M. Cossi, N. Rega, J. M. Millam, M. Klene, J. E. Knox, J. B. Cross, V. Bakken, C. Adamo, J. Jaramillo, R. Gomperts, R. E. Strat- mann, O. Yazyev, A. J. Austin, R. Cammi, C. Pomelli, J. W. Ochterski, R. L. Martin, K. Morokuma, V. G. Zakrzewski, G. A. Voth, P. Salvador, J.J. Dan- nenberg, S. Dapprich, A. D. Daniels, O. Farkas, J.B. Foresman, J. V. Ortiz, J. Cioslowski, D. J. Fox, Gaussian, Inc., Wallingford CT, 2010.)
- [32] (A. D. Becke, *J. Chem. Phys.* **1993**, *98*, 5648-5652.
- [33] (G. A. Petersson, A. Bennett, T. G. Tensfeldt, M. A. Al-Laham, W. A. Shirley, J. Mantzaris, *J. Chem. Phys.* **1988**, *89*, 2193-2218.
- [34] (P. J. Hay, W. R. Wadt, *J. Chem. Phys.* **1985**, *82*, 299-310.)
- [35] R. Ditchfield, W. J. Hehre, J. A. Pople, *J. Chem. Phys.* **1971**, *54*, 724-728)
- [36] ([a] S. Grimme, J. Antony, S. Ehrlich, H. Krieg, *J. Chem. Phys.* **2010**, *132*, DOI 10.1063/1.3382344. [b] A. D. Becke, E. R. Johnson, *J. Chem. Phys.* **2005**, *123*, 154101. [c] S. Grimme, S. Ehrlich, L. Goerigk, *J. Comput. Chem.* **2011**, *32*, 1456-1465.)
- [37] (P. Tarakeshwar, D. Finkelstein-Shapiro, S. J. Hurst, T. Rajh, V. Mujica, *J. Phys. Chem. C* **2011**, *115*, 8994-9004)
- [38] (J. P. Perdew, K. Burke, M. Ernzerhof, *Phys. Rev. Lett.* **1996**, *77*, 3865-3868)
- [39] (W. Kutzelnigg, U. Fleischer, M. Schindler, in *NMR Basic Principles and Progress*, Vol. 23, Springer, Berlin, 1990, p.165.)

WILEY-VCH

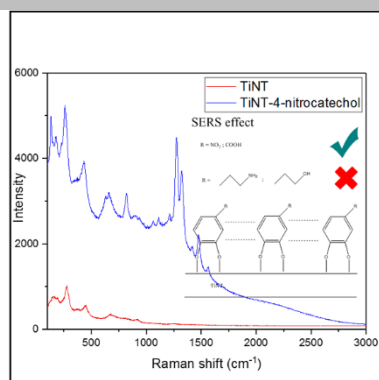
---

**Entry for the Table of Contents** (Please choose one layout)

Layout 1:

**FULL PAPER**

The SERS of trititanate nanotubes modified with enediol ligands was found to be dramatically affected by the functional group. When 4-nitrocatechol is attached an enhancement is seen; however, when dopamine is attached, no signal is seen. The relative band gap positions upon 785 nm laser excitation are proposed to explain the observed phenomenon



*Ruochen Liu, Edmund Morris,  
Xiaorong Cheng, Eric Amigues, Kim  
Lau, Baekman Kim, Yuanhang Liu,  
Zhipeng Ke, Sharon E. Ashbrook,  
Michael Bühl and Graham Dawson\**

**Page No. – Page No.****Title**

Layout 2:

**FULL PAPER**

((Insert TOC Graphic here; max. width: 11.5 cm; max. height: 2.5 cm))

*Author(s), Corresponding Author(s)\****Page No. – Page No.****Title**

Text for Table of Contents